Phonon self-energy in superconductors: Effect of vibrating impurities

A. Sergeev,* Ch. Preis, and J. Keller
Institut für Theoretische Physik, Universität Regensburg, D-93040 Regensburg, Germany
(Received 30 March 1999; revised manuscript received 6 October 1999)

The phonon self-energy due to the interaction with electrons is studied for superconductors with *s*- and *d*-wave pairing. Addition of impurities not only changes the electronic states, but it also generates a channel of the electron-phonon interaction due to electron scattering from vibrating impurities. Impurity-induced electron-phonon coupling results in significant modifications of the phonon self-energy. For a *d*-wave superconductor the phonon attenuation coefficient (the imaginary part of the phonon self-energy) has been calculated in the Born approximation and in the unitary limit for electron-impurity scattering. In the case of weak electron-impurity potential, the attenuation decreases if temperature reduces below T_c, while an increase of the attenuation in the superconducting state has been found in the unitary limit. The theory shows a good agreement with measured disorder-dependent coupling of the B_{1g} phonon mode to superconducting electrons in high-T_c samples: the Born approximation well describes temperature dependence of the attenuation in YBaCuO single crystals, the unitary limit corresponds to polycrystals and twinned crystals.

I. INTRODUCTION

Since the discovery of high-temperature superconductors, the interaction of optical phonons and electrons in these materials has been attracting much attention. Due to the low concentration of charge carriers, *c*-axis polarized optical phonons can be observed in Raman scattering and infrared reflection. Raman and IR spectroscopy make it possible to determine the spectrum and the attenuation of phonon modes, the superconducting gap position, and also some characteristics of electron states (such as electron scattering rate). These measurements turned out to be a very useful probe of phonons, the electron-phonon interaction, and superconductivity. Up to now there are many papers devoted to these and related topics.[1–6]

In this paper, we will focus on impurity-induced coupling of optical phonons and electrons. Because the high-T_c oxides become superconducting under doping, the electron-impurity scattering generated by the substitutional disorder is very important even in single crystals. Impurities play a twofold role in the electron-phonon interaction. First, addition of impurities modifies the electron states in a superconductor. This modification of electron states results in significant changes in the superconductivity-induced phonon self-energy effects.[2] Second, electron scattering from vibrating impurities (inelastic electron-impurity scattering) generates a new channel of the electron-phonon interaction. Note, that in the normal state impurity-induced coupling of acoustical phonons and electrons drastically changes all transport coefficients (temperature-dependent resistivity, thermopower, thermal conductivity) and electron-phonon dephasing rate.[7,8]

Due to the two different effects of impurities, one should distinguish between impurities vibrating with a given phonon mode, and impurities, which are external with respect to this phonon mode. External impurities may only change electron states due to elastic electron-impurity scattering. The effect of modification of electron states on optical phonons has been considered for a superconductor with *s* pairing in Refs. 2–4. This effect is expected to be more significant in a *d*-wave superconductor, where the density of electron states is very sensitive to the electron-impurity scattering.[9]

The effect of vibrating impurities on phonon damping was studied in Ref. 10. If all impurities vibrate with the phonon mode under consideration, it is convenient to treat the electron-phonon interaction in the frame of reference, moving together with the lattice.[11] In this frame, impurities are motionless and therefore calculations are simplified.[10] However, such an approach is not applicable in the general case, and we should return to the description of the electron-phonon interaction in the ordinary frame.

In the present paper we study the phonon self-energy due to inelastic electron-impurity scattering for *s*- and *d*-wave superconductors (the modification of electron states is also taken into account). The paper is arranged as follows. In the next section we consider the impurity-induced interaction of normal electrons and optical phonons. In Secs. III and IV we calculate phonon attenuation due to vibrating impurities in *s*- and *d*-wave superconductors, correspondingly. In the Conclusions, we summarize our main results and suggest an interpretation of experimental data. In the Appendix, we show that a set of results may be reproduced in the comoving frame.

II. NORMAL STATE

Employing the Keldysh diagrammatic technique, we describe the electron system by the matrix Green function with retarded ($G_{21}=G^R$), advanced ($G_{12}=G^A$), and kinetic ($G_{22}=G^K$) components. If elastic electron-impurity scattering is taken into account, electron Green functions are

$$G_0^R(\mathbf{p},\epsilon)=[G_0^A(\mathbf{p},\epsilon)]^*=(\epsilon-\xi_p+i/2\tau)^{-1}, \tag{1}$$

$$G_0^K(\mathbf{p},\epsilon)=S_0(\epsilon)[G_0^A(\mathbf{p},\epsilon)-G_0^R(\mathbf{p},\epsilon)], \tag{2}$$

where $\xi_p=(p^2-p_F^2)/2m$, and $S_0(\epsilon)=-\tanh(\epsilon/2T)$ is the equilibrium distribution function, and τ is the electron-momentum relaxation time due to elastic electron-impurity scattering. We will calculate the phonon-electron self-energy

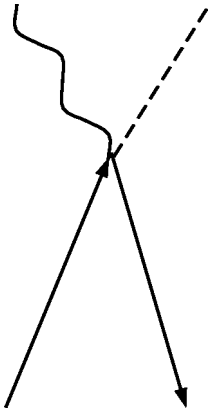

FIG. 1. Vertex $\hat{\gamma}_{in}$ taking into account electron scattering from vibrating impurities. In self-energy diagrams the solid, wavy, and dashed lines represent the electron, phonon, and impurity propagators, correspondingly.

in the first order in the electron-phonon interaction, therefore, phonon corrections in the electron Green functions may be ignored.

Inelastic electron-impurity scattering (electron scattering from vibrating impurities) is described by the Hamiltonian[12,13]

$$H_{int}=\sum_{\mathbf{p},\mathbf{k},\mathbf{q},n,\mathbf{R}_0}\gamma_{in}(\mathbf{k},\mathbf{q},n)c^{\dagger}_{\mathbf{p}}c_{\mathbf{p}-\mathbf{k}}(b_{\mathbf{q},n}+b^{\dagger}_{-\mathbf{q},n})\times\exp[-i(\mathbf{k}-\mathbf{q})\mathbf{R}_0], \tag{3}$$

where $c^{\dagger}_{\mathbf{p}}$ is the creation operator of an electron with momentum $\mathbf{p}$, $b^{\dagger}_{\mathbf{q},n}$ is the creation operator of a phonon with a wave vector $\mathbf{q}$ and polarization index n, $\mathbf{R}_0$ are the equilibrium impurity positions. The vertex of the inelastic electron-impurity scattering (see Fig. 1) is

$$\gamma_{in}(\mathbf{k},\mathbf{q},n)=-iV_{e-im}\frac{\mathbf{k}\mathbf{e}_n}{(2\rho\omega)^{1/2}}, \tag{4}$$

where V_{e-im} is the impurity scattering potential, e_n is the phonon polarization vector, ρ is the density. In the Keldysh technique the vertex $\gamma_{in}(\mathbf{k},\mathbf{q},n)$ is multiplied by the tensor K^k_{ij} [$K^1_{ij}=\delta_{ij}/\sqrt{2}$, and $K^2_{ij}=(\sigma_x)_{ij}/\sqrt{2}$] with an upper phonon index and lower electron indices. Note, that the inelastic electron-impurity scattering is characterized by a large value of the transferred momentum ($k\sim p_F$), while the transferred energy is the same as in the ''pure'' electron-phonon interaction. It is convenient to introduce the effective vertex $\hat{\Gamma}$ shown in Fig. 2, with the matrix components

$$\Gamma^1_{22}=-\Gamma^1_{11}=-\Gamma,$$

$$\Gamma^2_{11}=[S_0(\epsilon)-S_0(\epsilon+\omega)]\Gamma,$$

$$\Gamma^1_{12}=S_0(\epsilon)\Gamma,$$

$$\Gamma^2_{12}=\Gamma^2_{21}=\Gamma^2_{22}=0,$$

$$\Gamma^1_{21}=-S_0(\epsilon+\omega)\Gamma, \tag{5}$$

and

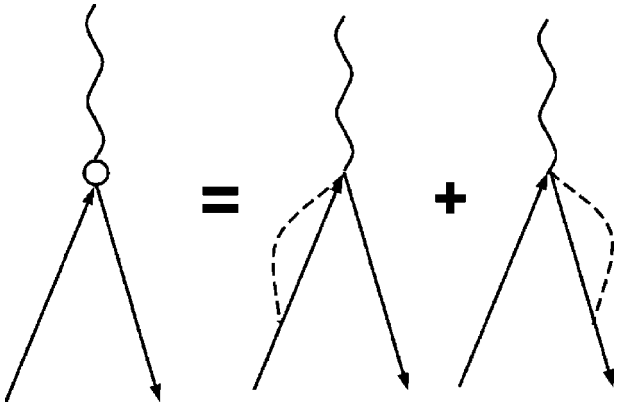

FIG. 2. Effective vertex $\hat{\Gamma}$, taking into account electron scattering from vibrating impurities.

$$\Gamma=\frac{\mathbf{p}\mathbf{e}_n}{2\tilde{\tau}(\rho\omega)^{1/2}}. \tag{6}$$

Here we express the electron-impurity potential through the corresponding electron-momentum relaxation rate

$$\tilde{\tau}^{-1}=\pi\nu(0)N_{im}V^2_{e-im}, \tag{7}$$

where $\nu(0)$ is the two-spin electron density of states, and N_{im} is the concentration of impurities vibrating with the phonon mode under consideration.

The phonon attenuation coefficient α is given by the retarded phonon self-energy P^R as $\alpha=-2\,\mathrm{Im}\,P^R$. We will calculate the attenuation coefficient of phonons with a small value of the wave vector, $q<q_0=\omega/v_F$. Due to the vector character of the vertex $\hat{\Gamma}$, it is not renormalized by the electron-impurity interaction and also is not screened.

The phonon self-energy diagrams generated by electron scattering from vibrating impurities are shown in Fig. 3. The contribution of the first diagram in the normal state to the attenuation coefficient is independent on the parameter $\omega\tau$ and it is given by[10]

$$\alpha_1=\frac{p_F^2\nu(0)}{3\tilde{\tau}\rho}. \tag{8}$$

In the normal state the second diagram with effective vertices $\hat{\Gamma}$ is formally given by

$$P^R=-2i\int\frac{d\mathbf{p}}{(2\pi)^3}\frac{d\epsilon}{2\pi}\Gamma^1_{22}(\mathbf{q},\omega)G^A_0(\mathbf{p},\epsilon)\times G^R_0(\mathbf{p}+\mathbf{q},\epsilon+\omega)\Gamma^2_{11}(-\mathbf{q},-\omega). \tag{9}$$

Evaluating Eq. (9), we find that the contribution of the second diagram is

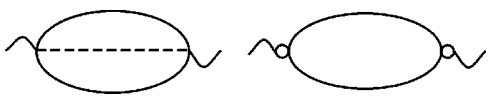

FIG. 3. Phonon self-energy diagrams due to vibrating impurities.

$$\alpha_2 = -\frac{p_F^2 \nu(0)}{3\rho\tilde{\tau}} \frac{\tau}{\tilde{\tau}} \mathrm{Re}(1+i\omega\tau)^{-1}. \quad (10)$$

Thus, the attenuation coefficient given by both diagrams is

$$\alpha_n = \frac{p_F^2 \nu(0)}{3\rho\tilde{\tau}} \left[1 - \frac{\tau/\tilde{\tau}}{1+(\omega\tau)^2} \right]. \quad (11)$$

In the pure case, $\omega\tau \gg 1$, α_2 is negligible and the phonon attenuation due to electron scattering from vibrating impurities is given by Eq. (8). If $\omega\tau \ll 1$, and all impurities vibrate with the phonon mode under consideration ($\tau = \tilde{\tau}$), the attenuation coefficient is

$$\alpha_n^* = \frac{p_F^2 \nu(0) \tau \omega^2}{3\rho}. \quad (12)$$

For completeness, we mention that, if impurities do not vibrate with the phonon mode under consideration, the self-energy of optical phonons has the Drude form, i.e., it is proportional to $-\nu(0)/(1-i\omega\tau)$.[2–4]

III. ISOTROPIC *s*-WAVE SUPERCONDUCTOR

In the superconducting state the electron Green function is given by

$$\hat{G}_0^{R,A} = \frac{1}{\xi_p^2 - (\xi^{R,A})^2} (-\xi_p \hat{\sigma}_z - \epsilon^{R,A} \hat{\sigma}_0 + \Delta^{R,A} \hat{\sigma}_x), \quad (13)$$

where σ's are the Pauli matrices in the Nambu space.

For an *s*-wave superconductor, electron-impurity scattering is taken into account by the equations

$$\epsilon^R = \epsilon + i\epsilon^R/(2\tau\xi^R),$$

$$\Delta^R = \Delta + i\Delta^R/(2\tau\xi^R),$$

$$(\xi^R)^2 = (\epsilon^R)^2 - (\Delta^R)^2. \quad (14)$$

As in the normal state, in the pure case, $\omega, \Delta \gg 1/\tau$, the main contribution to the phonon attenuation is given by the first diagram in Fig. 3. In the superconducting state the vertex γ_{in} carries the Nambu matrix σ_z. Therefore, the corresponding equation for P^R in the superconducting state has the form

$$\mathrm{Im}\, P^R = \mathrm{Sp}\ \ \mathrm{Re}\frac{1}{2}\int \frac{d\mathbf{p}}{(2\pi)^3} \frac{d\mathbf{p}'}{(2\pi)^3} \frac{d\epsilon}{2\pi} (S_+ - S) |\gamma_{in}|^2$$

$$\times \hat{\sigma}_z [\hat{G}_0^A \hat{\sigma}_z (\hat{G}_0^R)_+ - \hat{G}^R \hat{\sigma}_z (\hat{G}_0^R)_+], \quad (15)$$

where $(\hat{G}_0)_+ = \hat{G}(\mathbf{p}', \epsilon+\omega)$, and $S_+ = S(\epsilon+\omega)$.

Taking into account that $\epsilon^R/\xi^R = \epsilon/\xi$ and $\Delta^R/\xi^R = \Delta/\xi$, where $\xi = (\epsilon^2 - \Delta^2)^{1/2} \mathrm{sgn}(\epsilon) \Theta(|\epsilon| - |\Delta|)$, we find the attenuation of the optical phonon in an *s*-wave superconductor α_s,

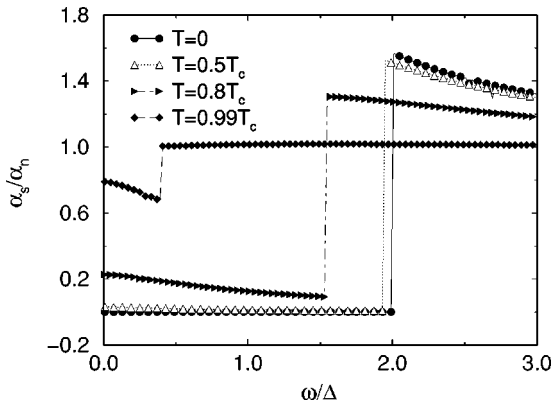

FIG. 4. Frequency dependency of the attenuation coefficient in the Born limit for *s*-wave symmetry of the order parameter.

$$\frac{\alpha_s}{\alpha_n} = \left(\int_{-\infty}^{-\omega-\Delta} + \int_{\Delta}^{\infty} + \theta(\omega - 2\Delta) \int_{-\omega+\Delta}^{-\Delta} \right) d\epsilon$$

$$\times \frac{S - S_+}{2\omega} \left(\frac{\epsilon\epsilon_+}{\xi\xi_+} - \frac{\Delta^2}{\xi\xi_+} \right), \quad (16)$$

where $\epsilon_+ = \epsilon + \omega$, $\xi_+ = \xi(\epsilon+\omega)$. The attenuation coefficient in the normal state α_n is given by Eq. (8).

As it is seen from Eq. (16), the impurity-induced attenuation of optical phonons is described by the same equation as the high-frequency ultrasonic attenuation.[14] For comparison with *d*-wave pairing, which will be discussed in Sec. IV, we present the ratio of α_s/α_n, as a function of frequency in Fig. 4. A discontinuity in the attenuation of phonons appears, when the frequency is equal to the energy gap.

Now we consider the impure case: $\omega, \Delta \ll 1/\tau$. Here we have to take into account also the second diagram in Fig. 3. The matrix elements of the effective vertex Γ in the superconducting state are

$$\Gamma_{22}^1 = (1/2)(\Gamma_+ + \Gamma),$$

$$\Gamma_{22}^2 = 0,$$

$$\Gamma_{12}^1 = S_0(\epsilon)\Gamma,$$

$$\Gamma_{12}^2 = (1/2)(\Gamma_+ - \Gamma),$$

$$\Gamma_{21}^1 = -S_0(\epsilon+\omega)\Gamma_+,$$

$$\Gamma_{21}^2 = -(1/2)(\Gamma_+ - \Gamma),$$

$$\Gamma_{11}^1 = -(1/2)(\Gamma_+ - \Gamma),$$

$$\Gamma_{11}^2 = \Gamma_{12}^1 + \Gamma_{21}^1, \quad (17)$$

where

$$\Gamma(\epsilon) = \left(\frac{\epsilon}{\xi} \hat{\sigma}_0 + \frac{\Delta}{\xi} \hat{\sigma}_x \right) \frac{\mathbf{p}\mathbf{e}_n}{2\tilde{\tau}(\rho\omega)^{1/2}}, \quad (18)$$

and $\Gamma_+ = \Gamma(\epsilon_+)$.

Therefore, the contribution of the second diagram is found to be

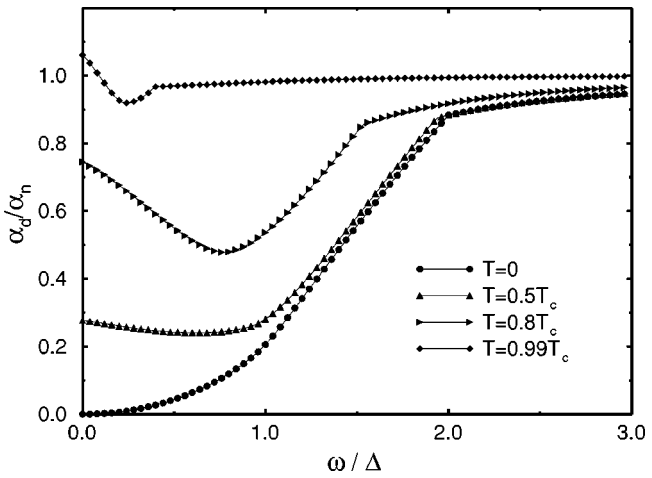

FIG. 5. Frequency dependency of attenuation coefficient in the Born limit for *d*-wave symmetry of the order parameter.

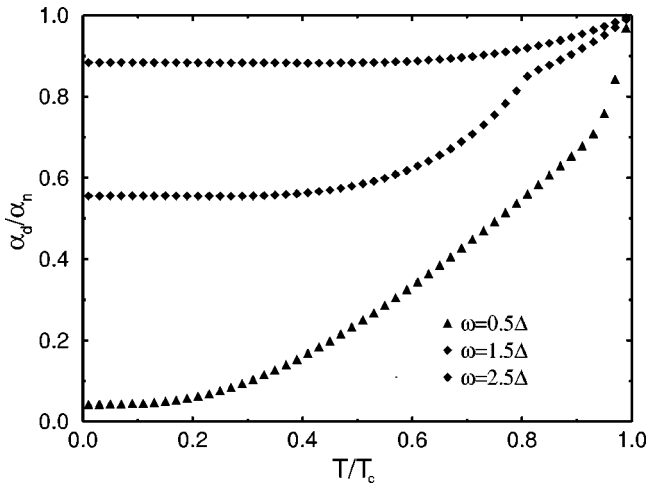

FIG. 6. Temperature dependency of attenuation coefficient in the Born limit for *d*-wave symmetry of the order parameter.

$$\mathrm{Im}\,P_2^R = \mathrm{Sp}\ \ \mathrm{Re}\frac{1}{4}\int \frac{d\mathbf{p}}{(2\pi)^3}\frac{d\epsilon}{2\pi}(S-S_+)[(\hat{\Gamma}_+ + \hat{\Gamma}) \times \hat{G}_0^A(\hat{\Gamma}_+ + \hat{\Gamma})(\hat{G}_0^R)_+ - (\hat{\Gamma}_+ - \hat{\Gamma}) \times \hat{G}_0^R(\hat{\Gamma}_+ - \hat{\Gamma})(\hat{G}_0^R)_+], \tag{19}$$

where $(\hat{G}_0)_+ = \hat{G}(\mathbf{p}, \epsilon+\omega)$.

In the general case the equation for α_s is complicated. If all impurities vibrate with the phonon mode under consideration ($\tau = \tilde{\tau}$), the large contribution of the first diagram [Eq. (15)] is canceled by the leading term of the second diagram. The rest of the second diagram is

$$\frac{\alpha_s}{\alpha_n^*} = \left(\int_{-\infty}^{-\omega-\Delta} + \int_{\Delta}^{\infty} + \theta(\omega-2\Delta)\int_{-\omega+\Delta}^{-\Delta}\right) d\epsilon \times \frac{S-S_+}{2\omega}\left(\frac{\epsilon\epsilon_+}{\xi\xi_+} + \frac{\Delta^2}{\xi\xi_+}\right), \tag{20}$$

where α_n^* is given by Eq. (12). As it is seen, Eq. (20) differs only in a sign in the coherence factor from Eq. (16). So the impurity-induced attenuation of optical phonons in the limiting cases is described by BCS relations with different coherence factors. The function given by Eq. (20) is well known (see Ref. 15).

IV. *d*-WAVE SUPERCONDUCTOR

Keeping in mind that the momentum relaxation rate in high-T_c oxides corresponds to the pure case ($\omega, \Delta_0 \gg 1/\tau$), we consider here only this limit. We assume pairing of *d*-wave symmetry $\Delta(\mathbf{p}) = \Delta_0 \cos(2\phi)$ in planes, which are perpendicular to the *c* axis.

In this model the angular averaged value of the order parameter Δ is zero, and Δ is not renormalized by electron-impurity scattering ($\mathrm{Im}\,\Delta = 0$). This simplifies the calculations significantly. The Born approximation for electron-impurity scattering results in the relations[16]

$$\epsilon^R = \epsilon + (i/2\tau)\langle \epsilon/\xi \rangle,$$

$$\Delta^R = \Delta,$$

$$\xi^R = \xi + (i/2\tau)(\epsilon/\xi)\langle \epsilon/\xi \rangle, \tag{21}$$

where $\langle\ \rangle$ stands for averaging over the direction of the electron momentum.

In the pure case, again the attenuation coefficient is determined by the first diagram in Fig. 3. For a phonon with polarization $\mathbf{e}_n$ parallel to the *c* axis, it may be presented as

$$\frac{\alpha_d}{\alpha_n} = \frac{\tau}{2}\int d\epsilon \frac{(S-S_+)}{\omega}(\rho_+\gamma + \rho\gamma_+), \tag{22}$$

where $\gamma = \mathrm{Im}\,\epsilon^R$, and $\rho = \mathrm{Re}(\epsilon^R/\xi^R)$ is the dimensionless superconducting density of states. In the Born limit, we obtain the attenuation coefficient given by

$$\frac{\alpha_d}{\alpha_n} = \frac{1}{2\omega}\int d\epsilon (S-S_+)\rho(\epsilon)\rho(\epsilon+\omega), \tag{23}$$

where the density of states for a *d*-wave superconductor is

$$\rho(\epsilon) = \frac{2}{\pi}\begin{cases} (\epsilon\Delta_0)K(\epsilon\Delta_0), & \text{if } \epsilon < \Delta_0 \\ K(\Delta_0\epsilon), & \text{if } \epsilon > \Delta_0, \end{cases} \tag{24}$$

where $K(x)$ is the complete elliptic integral of the first kind. Frequency and temperature dependencies of the attenuation coefficient are presented in Figs. 5 and 6. The kinks in the frequency and temperature dependencies correspond to $\omega = 2\Delta_0(T)$.

For resonant electron-impurity scattering (the unitary limit), the phonon self-energy diagrams are shown in Fig. 7. The self-energy may be presented again by Eq. (22) through the electron density of states ρ, and the electron damping $\gamma(\epsilon) = \mathrm{Im}\,\epsilon^R$ where one has to take into account that the resonant electron-impurity scattering results in the residual superconducting density of states at the Fermi energy:[9,17]

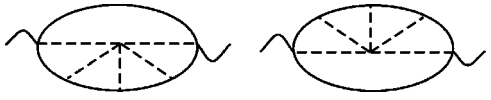

FIG. 7. Phonon self-energy diagrams in the unitary limit for electron-impurity scattering.

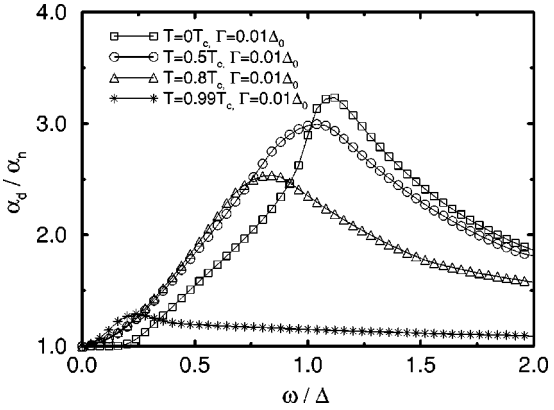

FIG. 8. Frequency dependency of attenuation coefficient in the unitary limit for *d*-wave symmetry of the order parameter.

$$\rho(0)=(2\gamma_0/\pi\Delta_0)\ln(4\Delta_0/\gamma_0), \tag{25}$$

where

$$\gamma_0^2=(\pi\Gamma\Delta_0/2)/\ln[4(2\Delta_0/\pi\Gamma)^{1/2}], \tag{26}$$

and 2Γ is the electron-momentum relaxation rate in the normal state in the unitary limit. In the energy scale $\epsilon\leqslant\gamma_0$, the self-consistent solution of the Dyson equation gives[5]

$$\epsilon^R=(1/2)\epsilon+i\gamma_0-i(\epsilon^2/8\gamma_0). \tag{27}$$

For higher energies $\epsilon\geqslant\gamma_0$, the self-consistency is not important, and $\gamma(\epsilon)=\Gamma/\rho(\epsilon)$, where $\rho(\epsilon)$ is approximately given by Eq. (24). The energy dependence of the electron density of states for different values of Γ has been calculated numerically in Refs. 18 and 19. Using results for the electron density of states, we obtain $\gamma(\epsilon)$, and calculate frequency and temperature dependencies of α_d/α_n. The results are shown in Figs. 8 and 9, respectively.

For small values of the electron-momentum relaxation rate Γ, the region $\epsilon\leqslant\gamma_0$ gives the main contribution to α_d. At $T=0$ we obtain the ratio of α_d/α_n to be larger than 1, which means a broadening of the phonon linewidth in the superconducting state. Moreover, we find a nonmonotonic temperature dependence of the attenuation in the unitary limit.

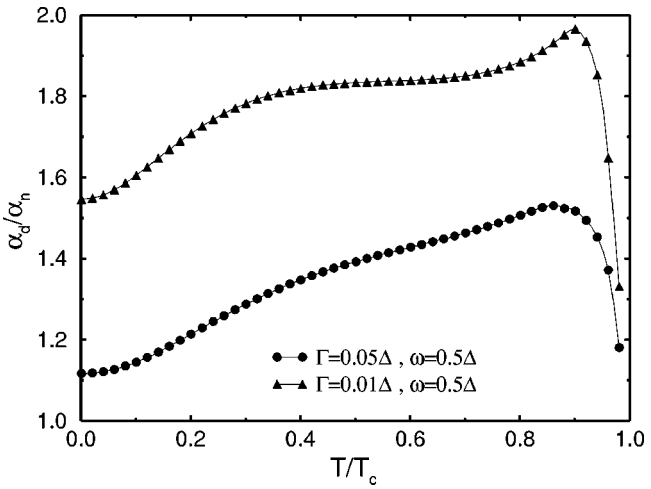

FIG. 9. Temperature dependency of attenuation coefficient in the unitary limit for *d*-wave symmetry of the order parameter.

V. CONCLUSIONS AND COMPARISON WITH EXPERIMENT

To summarize, we have studied the effect of vibrating impurities on the attenuation of optical phonons especially in the superconducting state. Inelastic electron scattering from vibrating impurities creates a channel of the phonon attenuation. Vibrating impurities result in significant change of the phonon self-energy and provide an important channel of phonon attenuation. This effect is thought to be relevant for high-T_c copper oxides.

We have found that in the normal state the attenuation induced by the vibrating impurities depends on the parameter $\omega\tau$ [Eq. (11)] due to elastic electron-impurity scattering. In the pure case, $\omega\tau\gg1$, the attenuation coefficient is independent on the phonon frequency.[8] Attenuation decreases with addition of external impurities. If all impurities vibrate with the phonon mode under consideration, the attenuation coefficient is proportional to ω^2 in the dirty limit $\omega\tau\ll1$ [Eq. (12)].

Our calculations show that for the *s*-wave superconductor the impurity-induced attenuation in the limiting cases is described by BCS relations with different coherence factors [Eqs. (16) and (20)]. In the pure case the coherence factor corresponds to the sound attenuation in the BCS theory. Phonon attenuation in the impure case depends on the character and position of impurities. If all impurities vibrate with the phonon mode under consideration, the coherence factor is the same as for electron interaction with an electromagnetic field. In the ordinary frame of reference (Sec. III), it is nontrivial consequence of the quantum interference between electron-phonon and electron-impurity scattering. Transformation to the comoving frame simplifies calculations (see the Appendix). The corresponding vertex of the electron-phonon interaction brings the same matrix in Nambu space as the interaction with an electromagnetic field.

In a *d*-wave superconductor the impurity-induced attenuation strongly depends on the value of the electron-impurity potential. In the case of weak electron-impurity scattering (the Born approximation) the attenuation coefficient at low temperatures decreases due to the superconducting transition (Figs. 5 and 6). Therefore, the phonon should acquire narrow linewidth in the superconducting state. However, in the case of strong electron-impurity scattering (the unitary limit) this result is altered. Strong scattering in *d*-wave superconductors simultaneously creates an impurity-induced channel of attenuation and modifies the electron states. In the unitary limit the attenuation increases in the superconducting state (Figs. 8 and 9).

The main features of our theoretical curves are supported by available data. The most significant changes in the phonon self-energy in the superconducting state are observed for a 340-cm^{-1} B_{1g}-like mode in YBaCuO samples.[1] This is not surprising, since O2–O3 plane-oxygen vibrations dominate in this mode. It is expected in our model that coupling of the 340-cm^{-1} mode with superconducting electrons is extremely sensitive to disorder. Raman measurements do show such

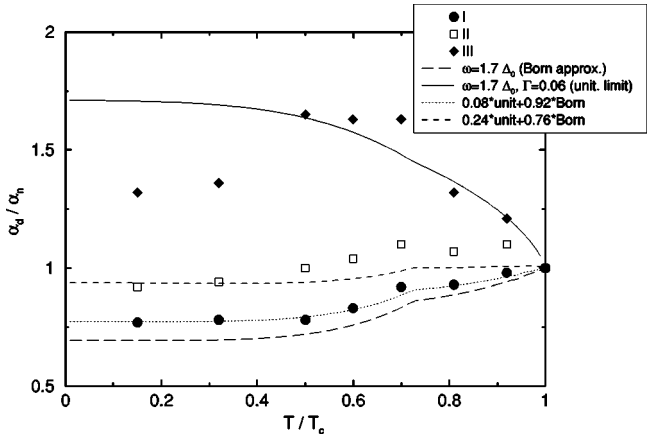

FIG. 10. Temperature dependency of attenuation coefficient measured in the detwinned crystal (●), the crystal with large untwinned areas (□), the heavily twinned sample (♦) (all data from Fig. 4 of Ref. 21) and theoretical curves of impurity-induced phonon attenuation in the superconductor with *d* pairing (Figs. 6 and 9).

intriguing behavior. The phonon linewidth in single crystals exhibit tremendous sharpening below T_c,[20,21] while a significant broadening is observed in polycrystalline samples and twinned crystals[1,21] (see Fig. 4 in Ref. 21).

Our interpretation of experimental results is as follows. In single superconducting YBaCuO crystals electrons scatter from the oxygen vacancies in CuO chains. The oxygen vacancy is known to present a weak scattering potential for electrons confined in the Cu-O plane.[9] Therefore, we expect that our results obtained in the Born approximation [Eq. (23) and Figs. 5 and 6] are applicable to this case. As we mentioned, the measured attenuation of the B_{1g} mode drastically decreases below the superconducting transition. Temperature dependencies observed in Refs. 20 and 21 are in a good agreement with our curves on Fig. 6. Note also, that according to Figs. 5 and 6 the effect of superconductivity on high-frequency modes is negligible. For this reason, the A_{1g} plane oxygen mode (440 cm^{-1}) in single crystals does not change within the precision of measurements.[21]

Polycrystals and twinned crystals of YBaCuO are well described by the resonant electron-impurity scattering.[9] For such samples our theory predicts the significant enhancement of the attenuation below T_c (see Figs. 8 and 9), which is in agreement with numerous experimental results.[1] At the same time, a relative change of the attenuation and a form of the temperature dependence show considerable changes from sample to sample.[1,21] In our formalism, this sensitivity to the sample quality results from the strong dependence of the superconducting density of states on elastic electron scattering in the unitary limit (Fig. 8).

By way of illustration we apply our model to experimental data from Ref. 21, Fig. 4. We rebuilt the experimental temperature dependencies of the YBaCuO 340-cm^{-1} phonon linewidth, $\alpha(T)$, in dimensionless coordinates α/α_n versus T/T_c, where $\alpha_n=\alpha(T_c)$. Figure 10 shows the relative change of the attenuation coefficient (phonon linewidth) for different samples: the perfect (detwinned) crystal (●), the crystal with large untwinned areas (□), the heavily twinned sample (♦), and a few theoretical curves of impurity-induced phonon attenuation in the superconductor with *d* pairing (Figs. 6 and 9). As seen, the temperature dependence of the phonon linewidth in the perfect crystal is well described by our model with weak electron-impurity scattering (the Born approximation). Note that we choose the value of Δ_0 to be 200 cm^{-1} that was reported in many papers. We do not use any fitting parameters for this theoretical curve. As we discussed, heavily twinned samples should be described by the unitary limit for electron-impurity scattering. According to our results (Figs. 8 and 9), in the unitary limit the linewidth depends on the parameter Γ. The theoretical curve with $\Gamma/\Delta_0=0.06$ is in good agreement with data obtained at $T>0.5T_c$. At the same time, with this value of Δ_0 we cannot explain low-temperature data. In the frame of our model, the nonmonotonic temperature dependence of α may be obtained only for $\omega\leqslant\Delta_0$ (see Figs. 8 and 9). This leads to relatively large values of Δ_0. Although such values have been reported, most experiments give the value of Δ_0 in the range from 170 to 250 cm^{-1}. As it is seen in Fig. 10, our model describes the transition from sharpening to broadening of the 340-cm^{-1} phonon line due to disorder enhancement; it gives a correct scale of the observed effects. More detailed theory should take into account energy dependence of scattering and density of states in the normal state of high-T_c materials.

The next important fact in favor of the impurity-induced electron-phonon coupling in high-T_c materials is that the oxygen disorder in chains has a very similar effect on the phonon linewidth as an introduction of heavy-metal impurities substituting Cu in the chains.[22,23]

To the best of our knowledge, there is no theory connecting the observed sharpening and broadening of phonon lines with quality of superconducting samples. The broadening of lines in the superconducting state is usually related to the Zeyher-Zwicknagl theory, which predicts superconductivity-induced coupling of the B_{1g} mode with electrons.[2–5,24] Assuming zone-center photons with $q=0$, this theory does not allow any phonon line to sharpen below T_c. In Ref. 6 the sharpening of some lines in single crystals is associated with nonzero wave vectors of phonons measured in Raman experiments.

We would like to note that in the current paper we have considered only the imaginary part of the electron-phonon self-energy in the superconducting state. Addition of impurities also significanly changes a spectrum of the lattice vibrations.[25] Calculating the phonon linewidth, we assume that the effect of impurities on the phonon spectrum is already taken into account. We also ignore additional modification of the phonon spectrum in the superconducting state. Experiments show that the relative spectrum changes due to superconductivity are small; in particular, for the 340-cm^{-1} line, the shift $\Delta\nu$ is 8 cm^{-1}. Additional corrections to the imaginary part of the self-energy due to the shift of phonon frequency may be obtained in first order in small parameter $\Delta\nu/\nu\sim 0.02$.

The vibrating potential of impurities, defects, and boundaries plays an important role in many nonequilibrium and transport phenomena, such as electron cooling and dephasing,[13,26] electrical conductivity,[7] Kapitza resistance,[8] and thermopower.[8] Arguments presented in this section show evidence about significant electron-phonon coupling due to

vibrating dopants and defects in high-T_c superconductors. In order to differentiate between different mechanisms of electron-phonon coupling in copper oxides, more theoretical and experimental investigations have to be done. In particular, study of the phonon linewidth depending on the electron-momentum relaxation rate and the residual superconducting density of electron states would be useful to evaluate parameter Γ and impurity-induced electron-phonon coupling.

ACKNOWLEDGMENTS

The support by the Alexander von Humboldt Foundation, Graduiertenkolleg, and Bayerische Forschungsstiftung is greatly acknowledged.

APPENDIX: COMOVING FRAME

As we discussed in the Introduction, using the comoving frame provides us with a convenient description of the electron-phonon interaction in an impure system, if all impurities vibrate with the phonon mode under consideration ($\tau = \tilde{\tau}$).

The bare vertex of the electron-phonon interaction in the comoving frame has a form[10,11]

$$\Gamma(\mathbf{p},\mathbf{q}) = \Gamma_1(\mathbf{p},\mathbf{q}) + \Gamma_2(\mathbf{p},\mathbf{q}), \tag{A1}$$

$$\Gamma_1(\mathbf{p},\mathbf{q}) = -i\frac{(\mathbf{p}\cdot\mathbf{q})(\mathbf{p}\cdot\mathbf{e}_\lambda)}{m(2\rho\omega_q)^{1/2}}\hat{\sigma}_z, \tag{A2}$$

$$\Gamma_2(\mathbf{p},\mathbf{q}) = -i\frac{\omega(\mathbf{p}\cdot\mathbf{e}_\lambda)}{(2\rho\omega)^{1/2}}\hat{1}. \tag{A3}$$

Vertices Γ_1 and Γ_2 carry different matrices $\hat{\sigma}_z$ and $\hat{1}$ in the Nambu space due to their different symmetry under the transformation $\mathbf{p}\rightarrow-\mathbf{p}$. For acoustic phonons the vertex Γ_2 is small compared with Γ_1. However, for optical phonons Γ_2 gives the leading contribution, when $q<q_0=\omega/v_F$ (v_F is the Fermi velocity).

Due to the vector character of the vertex Γ_2, it is not renormalized by the impurity ladder, if $q<q_0$. For the same reason, screening of the interaction described by Γ_2 results in small corrections. Therefore, when $q<q_0$, the attenuation of optical phonons is given by the phonon self-energy with two vertices Γ_2. The corresponding equation has the form

$$\mathrm{Im}\,P^R = \mathrm{Sp}\ \ \mathrm{Re}\frac{1}{2}\int\int\frac{d\mathbf{p}}{(2\pi)^3}\frac{d\epsilon}{2\pi}\Gamma_2(\mathbf{p},\mathbf{q})^2(S-S_+)$$
$$\times[\hat{G}_0^A(\hat{G}_0^R)_+ - \hat{G}_0^R(\hat{G}_0^R)_+]. \tag{A4}$$

Integrating the products of Green functions in Eq. (A4) over ξ_p, we get

$$\mathrm{Sp}\int d\xi_p\,\hat{G}_0^A(\hat{G}_0^R)_+ = \frac{\pi i}{\xi_+^R-\xi^A}\left(1+\frac{\epsilon^A\epsilon_+^R}{\xi^A\xi_+^R}+\frac{\Delta^A\Delta_+^R}{\xi^A\xi_+^R}\right), \tag{A5}$$

$$\mathrm{Sp}\int d\xi_p\,\hat{G}_0^R(\hat{G}_0^R)_+ = \frac{\pi i}{\xi_+^R+\xi^R}\left(1-\frac{\epsilon^R\epsilon_+^R}{\xi^R\xi_+^R}-\frac{\Delta^R\Delta_+^R}{\xi^R\xi_+^R}\right). \tag{A6}$$

For a s-wave superconductor, $\epsilon^R/\xi^R=\epsilon/\xi$ and $\Delta^R/\xi^R=\Delta/\xi$, therefore, Eqs. (A5) and (A6) may be presented as

$$\mathrm{Sp}\int d\xi_p\,\hat{G}_0^A(\hat{G}_0^R)_+ = \frac{\pi i}{\omega}\left(\frac{\epsilon_+}{\xi_+}+\frac{\epsilon}{\xi}\right)\left(1+\frac{i/\tau}{\xi_+-\xi}\right)^{-1}, \tag{A7}$$

$$\mathrm{Sp}\int d\xi_p\,\hat{G}_0^R(\hat{G}_0^R)_+ = \frac{\pi i}{\omega}\left(\frac{\epsilon_+}{\xi_+}-\frac{\epsilon}{\xi}\right)\left(1+\frac{i/\tau}{\xi_++\xi}\right)^{-1}. \tag{A8}$$

Then calculating $\mathrm{Im}\,P^R$ [Eq. (A4)] we obtain the phonon attenuation coefficient given by Eqs. (16) and (20).

To calculate the phonon attenuation coefficient in the d-wave superconductor it is convenient to simplify Eqs. (A5) and (A6), using the following relations, which are valid in the case of $\mathrm{Im}\Delta=0$:

$$1+\frac{\epsilon^A\epsilon_+^R}{\xi^A\xi_+^R}+\frac{\Delta^2}{\xi^A\xi_+^R} = \left(\frac{\epsilon_+^R}{\xi_+^R}+\frac{\epsilon^A}{\xi^A}\right)\frac{\xi_+^R-\xi^A}{\epsilon_+^R-\epsilon^A}, \tag{A9}$$

$$1-\frac{\epsilon^R\epsilon_+^R}{\xi^R\xi_+^R}-\frac{\Delta^2}{\xi^R\xi_+^R} = \left(\frac{\epsilon_+^R}{\xi_+^R}-\frac{\epsilon^R}{\xi^R}\right)\frac{\xi_+^R+\xi^R}{\epsilon_+^R-\epsilon^R}. \tag{A10}$$

Using Eqs. (A9) and (A10), one can obtain the attenuation coefficient given by Eq. (22).

*Present address: Dept. ECE, Wayne State University, Detroit, MI 48202.

[1] A.P. Litvinchuk, C. Thomsen, and M. Cardona, in *Physical Propeties of High Temperature Superconductors*, edited by D.M. Ginsberg (World Scientific, Singapore, 1993), Vol. IV, Chap. 6.

[2] R. Zeyher and G. Zwicknagl, Z. Phys. B: Condens. Matter **78**, 175 (1990).

[3] F. Marsiglio, R. Akis, and J.P. Carbotte, Phys. Rev. B **45**, 9865 (1992).

[4] E.J. Nicol and J.P. Carbotte, Phys. Rev. B **47**, 8205 (1993).

[5] E.J. Nicol, C. Jiang, and J.P. Carbotte, Phys. Rev. B **47**, 8131 (1993).

[6] T.P. Devereaux, Phys. Rev. B **50**, 10 287 (1994).

[7] N.G. Ptitsina, G.M. Chulkova, K.S. Il'in, A.V. Sergeev, F.S. Pochinkov, and E.M. Gershenzon, Phys. Rev. B **56**, 10 089 (1997); K.S. Il'in, N.G. Ptitsina, A.V. Sergeev, G.N. Gol'tsman, E.M. Gershenzon, B.S. Karasik, E.V. Pechen, and S.I. Krasnosvobodtsev, *ibid.* **57**, 15 623 (1998).

[8] M.Yu. Reizer, A.V. Sergeev, and J. Wilkins, Ann. Phys. (San Diego) **257**, 44 (1997); A.V. Sergeev, Phys. Rev. B **58**, R10 199 (1998).

[9] P.J. Hirschfeld, W.O. Putikka, and D.J. Scalapino, Phys. Rev. B **50**, 10 250 (1994).

[10] M.Yu. Reizer, Phys. Rev. B **38**, 10 398 (1988).

[11] T. Tsuneto, Phys. Rev. **121**, 402 (1961).

[12] G. Grunvald and K. Scharnberg, Z. Phys. **268**, 197 (1974).

[13] M.Yu. Reizer and A.V. Sergeev, Zh. Eksp. Teor. Fiz. **90**, 1056 (1986) [Sov. Phys. JETP **63**, 616 (1986)].

[14] V.M. Bobetic, Phys. Rev. **136**, A1535 (1964).

[15] M. Tinkham, *Introduction to Superconductivity* (McGraw-Hill, New York, 1975).

[16] Approximation given by Eq. (21) is not valid in the narrow en-

ergy interval near Δ_0. This region is not important in our calculations.

[17] M.J. Graf, S-K. Yip, J.A. Sauls, and D. Rainer, Phys. Rev. B **53**, 15 147 (1996).

[18] T. Hotta, J. Phys. Soc. Jpn. **62**, 274 (1993).

[19] Ye Sun and K. Maki, Phys. Rev. B **51**, 6059 (1995).

[20] K.F. McCarty, H.B. Radousky, J.Z. Liu, and R.N. Shelton, Phys. Rev. B **43**, 13 751 (1991).

[21] V.G. Hadjiev, C. Thomsen, A. Erb, G. Müller-Vogt, M.R. Koblischka, and M. Cardona, Solid State Commun. **80**, 643 (1991).

[22] C. Thomsen, B. Friedl, M. Cieplak, and M. Cardona, Solid State Commun. **78**, 727 (1991).

[23] K.F. McCarty, J.Z. Liu, Y.X. Jia, R.N. Shelton, and H.B. Radousky, Solid State Commun. **79**, 359 (1991).

[24] A. Bill, V. Hizhnyakov, and E. Sigmund, Phys. Rev. B **52**, 7637 (1995).

[25] A.S. Barker and A.J. Sievers, Rev. Mod. Phys. **47** (S2), FS1 (1975).

[26] A. Sergeev and V. Mitin, Phys. Rev. B **61**, 6041 (2000).